Supporting Information for

Improving the constraint on the M_w 7.1 2016 off-Fukushima shallow normal-faulting earthquake with the high azimuthal coverage tsunami data from the S-net wide and dense network: Implication for the stress regime in the Tohoku overriding plate

T. Kubota[1], H. Kubo[1], K. Yoshida[2], N. Y. Chikasada[1], W. Suzuki[1],
T. Nakamura[3], and H. Tsushima[4]

[1] National Research Institute for Earth Science and Disaster Resilience, Japan.

[2] Graduate School of Science, Tohoku University, Japan.

[3] Central Research Institute of Electric Power Industry, Japan.

Contents of this file

Introduction

Text S1 explains the procedure for the inversion analysis. Figure S1 shows the trade-off curve used to determine the weight of the smoothing constraint. Figure S2 is the result of the tsunami source inversion using the pressure waveforms. Figure S3 is the result of the grid-search analysis. The forward simulation of the tsunami waveforms based on the finite fault model is shown in Figures S4 and S5. Table S1 shows the unknown parameters searched in the grid-search analysis. The station locations of the OBPGs installed by Tohoku University are listed in Table S2.

Text S1

This text explains the procedure for the tsunami source modeling shown in Section 4. We first explain how to simulate the tsunami Green's function, which are the pressure change waveforms due to the tsunami and seafloor displacement at each OBPG caused by the displacement of the small region of seafloor. We distribute the small elements of the seafloor uplift (unit source elements) around the focal area (rectangular area in Figure 4a). The unit source element of the seafloor vertical displacement is given by

$$u_{ij}(x,y) = u_0 \left[\frac{1}{2} + \frac{1}{2}\cos\left(\frac{2\pi(x-x_i)}{L_x}\right)\right]\left[\frac{1}{2} + \frac{1}{2}\cos\left(\frac{2\pi(y-y_j)}{L_y}\right)\right]$$

$$\text{for} \qquad x_i - \frac{L_x}{2} \le x \le x_i + \frac{L_x}{2}, \ y_j - \frac{L_y}{2} \le y \le y_j + \frac{L_y}{2}, \qquad (S1)$$

which takes the maximum value of $u_0 = 1$ cm at (x_i, y_j). Here, L_x and L_y are the spatial extent of the unit source element along the x- and y-directions, respectively. We assume that $L_x = L_y = 4$ km. Each of the unit sources overlaps with adjacent unit sources with a horizontal interval of $\Delta L_x = L_x/2$ and $\Delta L_y = L_y/2$. The numbers of unit sources along the x-direction and y-directions are $N_x = 25$ and $N_y = 25$, respectively, and the total number of unit sources is $N = N_x \times N_y = 625$. The size of the analytical area where the unit sources are distributed is 50 km $\times$ 50 km.

Using the seafloor vertical displacement from the unit sources, we calculate tsunamis using the following procedure. We assume the initial sea-surface height change assuming that the sea-surface displacement is equal to the seafloor displacement. We then solve the linear dispersive tsunami equation (Saito et al., 2010; Saito, 2019) in Cartesian coordinates with the staggered grid in order to simulate tsunamis:

$$\frac{\partial M}{\partial t} + gh\frac{\partial \eta}{\partial x} = \frac{1}{3}h^2\frac{\partial^2}{\partial x \partial t}\left(\frac{\partial M}{\partial x} + \frac{\partial N}{\partial y}\right)$$

$$\frac{\partial N}{\partial t} + gh\frac{\partial \eta}{\partial y} = \frac{1}{3}h^2\frac{\partial^2}{\partial y \partial t}\left(\frac{\partial M}{\partial x} + \frac{\partial N}{\partial y}\right), \qquad (S2)$$

$$\frac{\partial \eta}{\partial t} = -\frac{\partial M}{\partial x} - \frac{\partial N}{\partial y}$$

where the variable η is the sea surface height anomaly (tsunami height), M and N are the velocity components integrated along the vertical direction over the seawater depth, h is the water depth, and g is the gravitational constant. For water depth h, we use the JTOPO30 data with a spatial resolution of 30 arcsec, provided by the Marine Information Research Center of the Japan Hydrographic Association (http://www.mirc.jha.jp/en/), interpolating the spatial interval of $\Delta x = \Delta y = 1$ km. We assume that the displacement occurs instantaneously, at time $t = 0$ s. The temporal interval of the calculation is $\Delta t = 1$ s. After the calculation, we subtract the pressure offset change due to the seafloor displacement (Tsushima et al., 2012), assuming that a seawater column height change of 1 cm H_2O is equal to a pressure change of 1 hPa. We finally apply the same bandpass filter to the simulated waveform as that applied to the observation.

In order to estimate the tsunami source, we use the time-derivative waveforms of the bandpass-filtered pressure waveforms for the inversion analysis ($\partial p/\partial t$, Figure 4c), because the time-derivative of the step signal becomes the impulse signal and thus does not contain the offset change, which can reduce the artificials due to the tsunami-irrelevant steps (Kubota, Suzuki et al., 2018). The data time window used for the modeling, which includes the main part of the tsunami (indicated by the blue traces in Figure 4c), is manually determined. We solve the following observation equation:

$$\begin{pmatrix} \mathbf{d} \\ \mathbf{0} \end{pmatrix} = \begin{pmatrix} \mathbf{H} \\ \alpha\mathbf{S} \end{pmatrix} \mathbf{m} \qquad\qquad \text{(S3)}$$

The data vector $\mathbf{d}$ consists of the time-derivative waveforms of the observed pressure $\partial p / \partial t$, and the matrix $\mathbf{H}$ consists of the time-derivative of the tsunami Green's functions. The vector $\mathbf{m}$ consists of the amounts of the displacement of the unit sources, which are the unknown parameters to be solved. The matrix $\mathbf{S}$ indicates the constraint for the spatial smoothing (e.g., Baba et al., 2006) and the parameter α is its weight. The goodness of the estimated source is evaluated using the variance reduction (VR):

$$\text{VR} = \left(1 - \frac{\Sigma_i \left(d_i^{\text{obs}} - d_i^{\text{cal}} \right)^2}{\Sigma_i \ d_i^{\text{obs}^2}} \right) \times 100 \ (\%) \qquad\qquad \text{(S4)}$$

where d_i^{obs} and d_i^{cal} are the i-th data of the observed and calculated time-derivative pressure waveforms, respectively. The smoothing weight α is determined based on the trade-off between the weight and the VR (Figure S1) in order to avoid both the overfitting and oversmoothing of data.
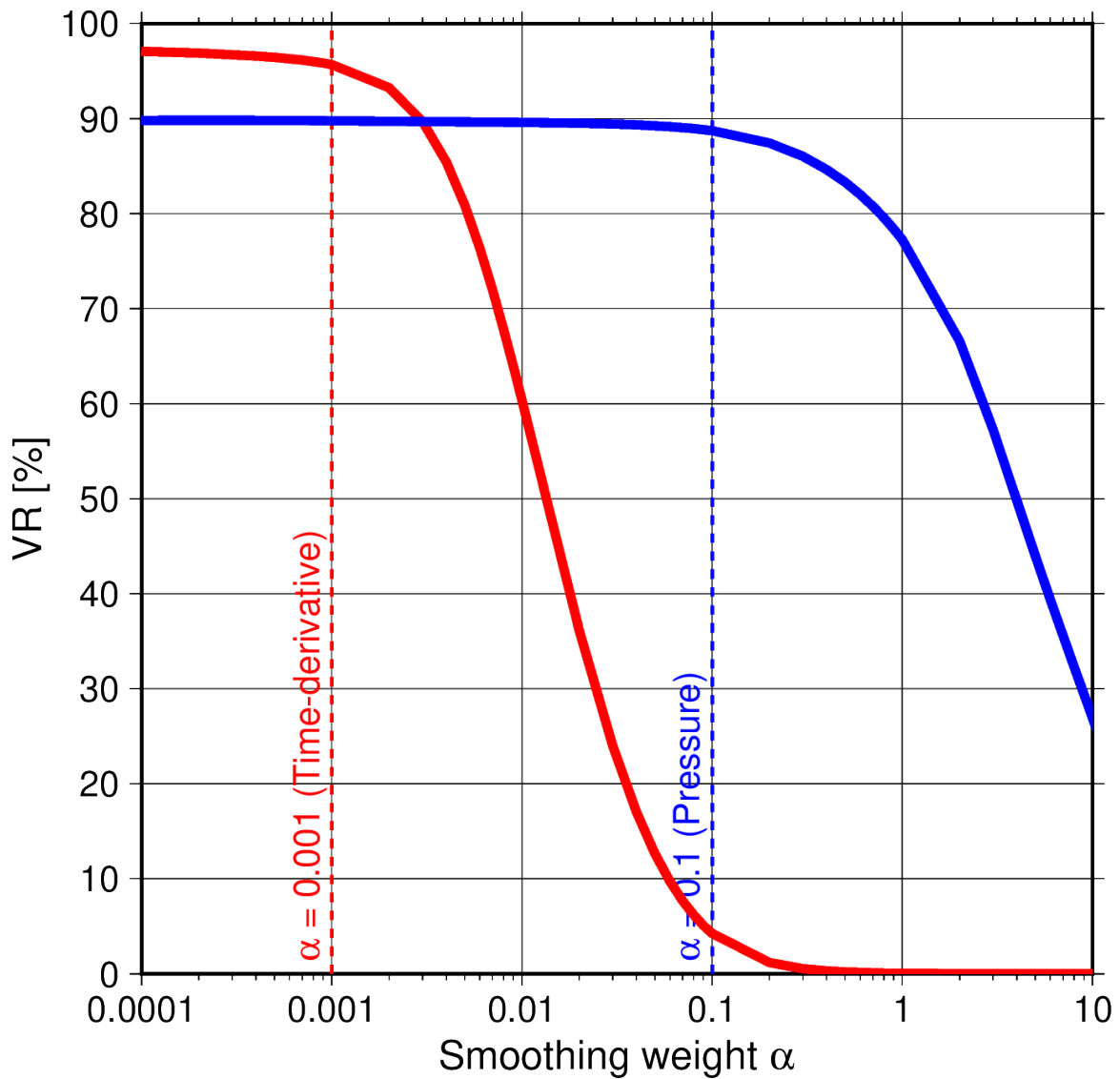
Figure S1. Trade-off curve between the smoothing weight *α* and VR. Red and blue solid lines are the trade-off curves for the inversions using the time-derivative waveform of the pressure (Figure 4) and the pressure waveform (Figure S2), respectively. Dashed lines denote the weight values used for the inversion analyses.
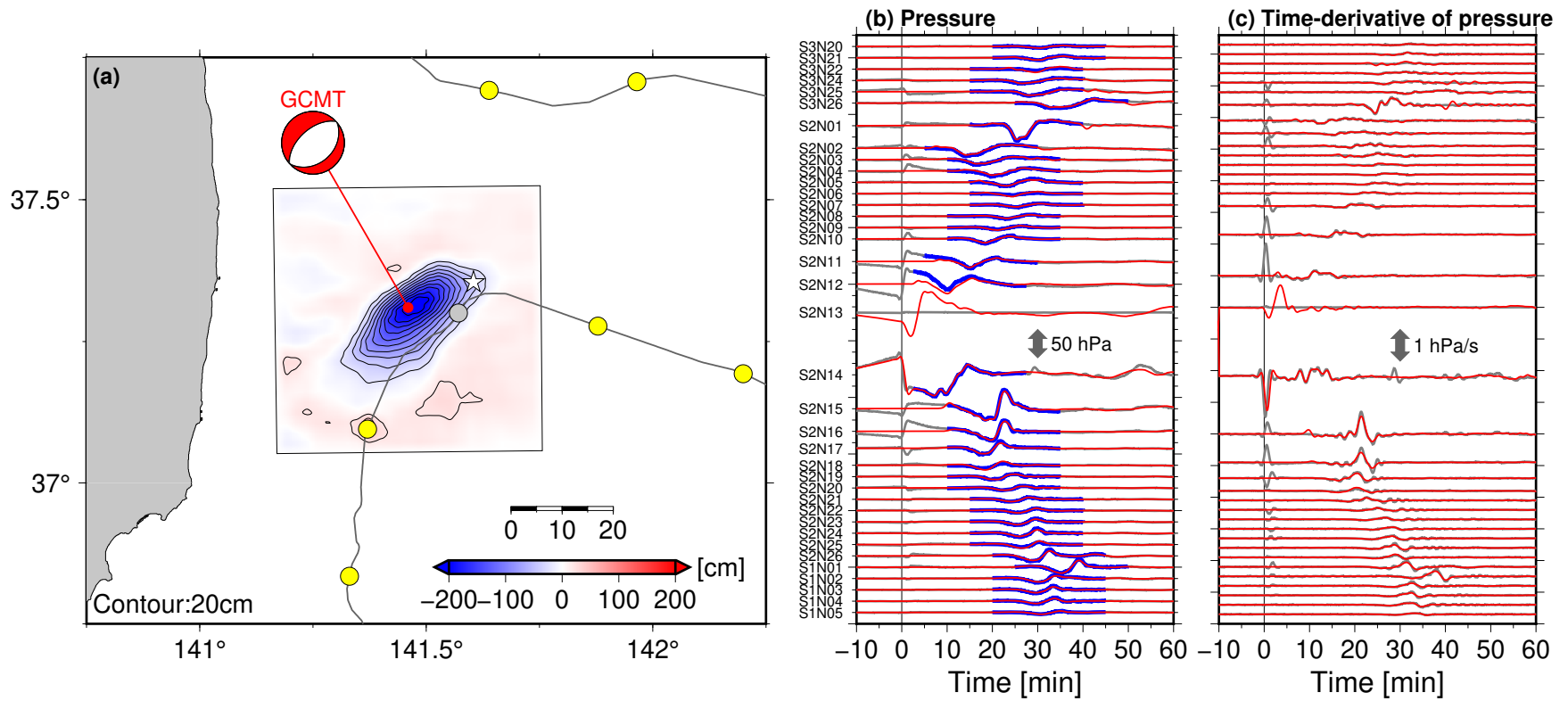
Figure S2. Results of the tsunami source inversion based on the conventional method. See Figure 4 for another explanation of this figure.
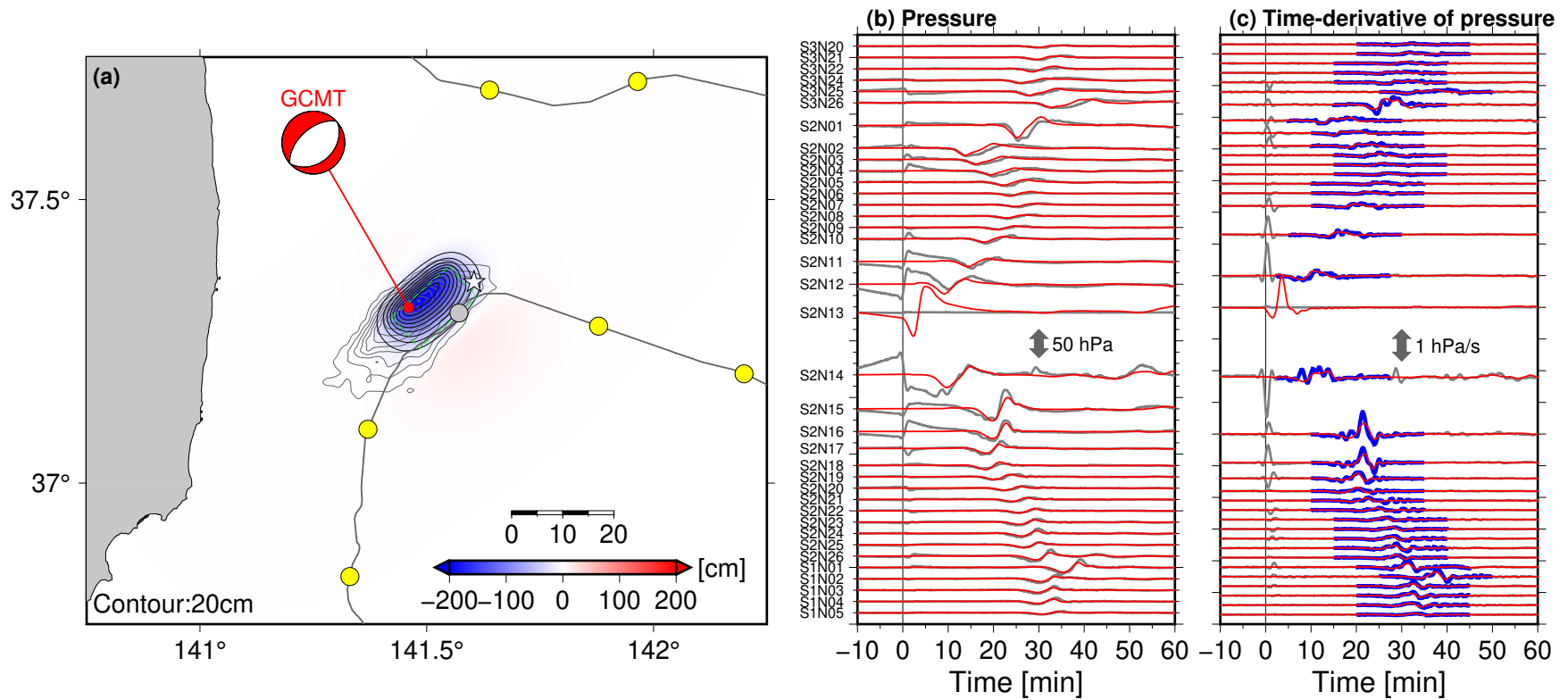
Figure S3. Results of the grid-search analysis. (a) Spatial distribution of the tsunami source. The green rectangle shows the location of the rectangular fault model. Comparisons of (b) the pressure waveforms and (c) the time-derivative waveforms. See Figure 4 for a detailed explanation of the figure.

2
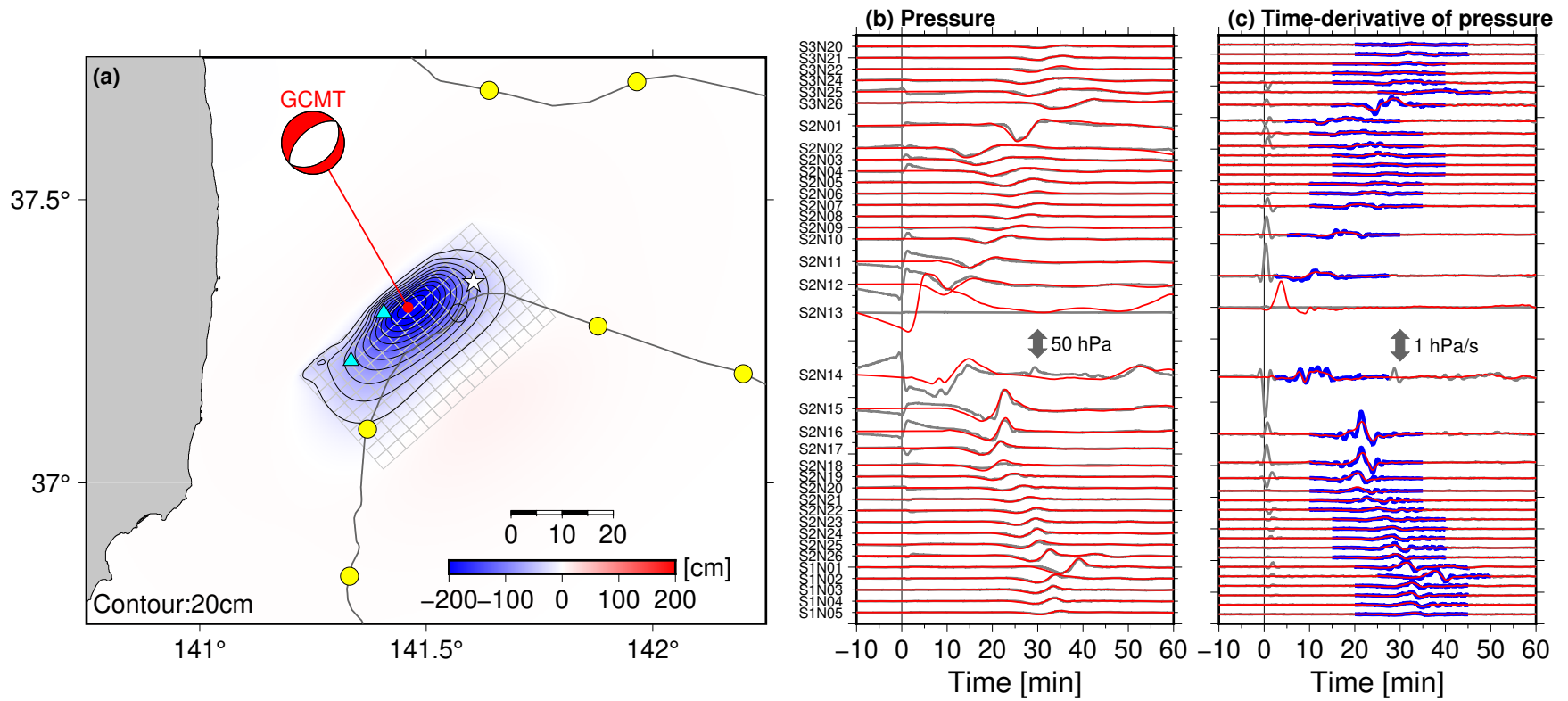
Figure S4. Results of the slip inversion. (a) Spatial distribution of the tsunami source calculated from the slip distribution in Figure 8a. Comparisons of (b) the pressure waveforms and (c) the time-derivative waveforms. See Figure 4 for a detailed explanation of the figure.
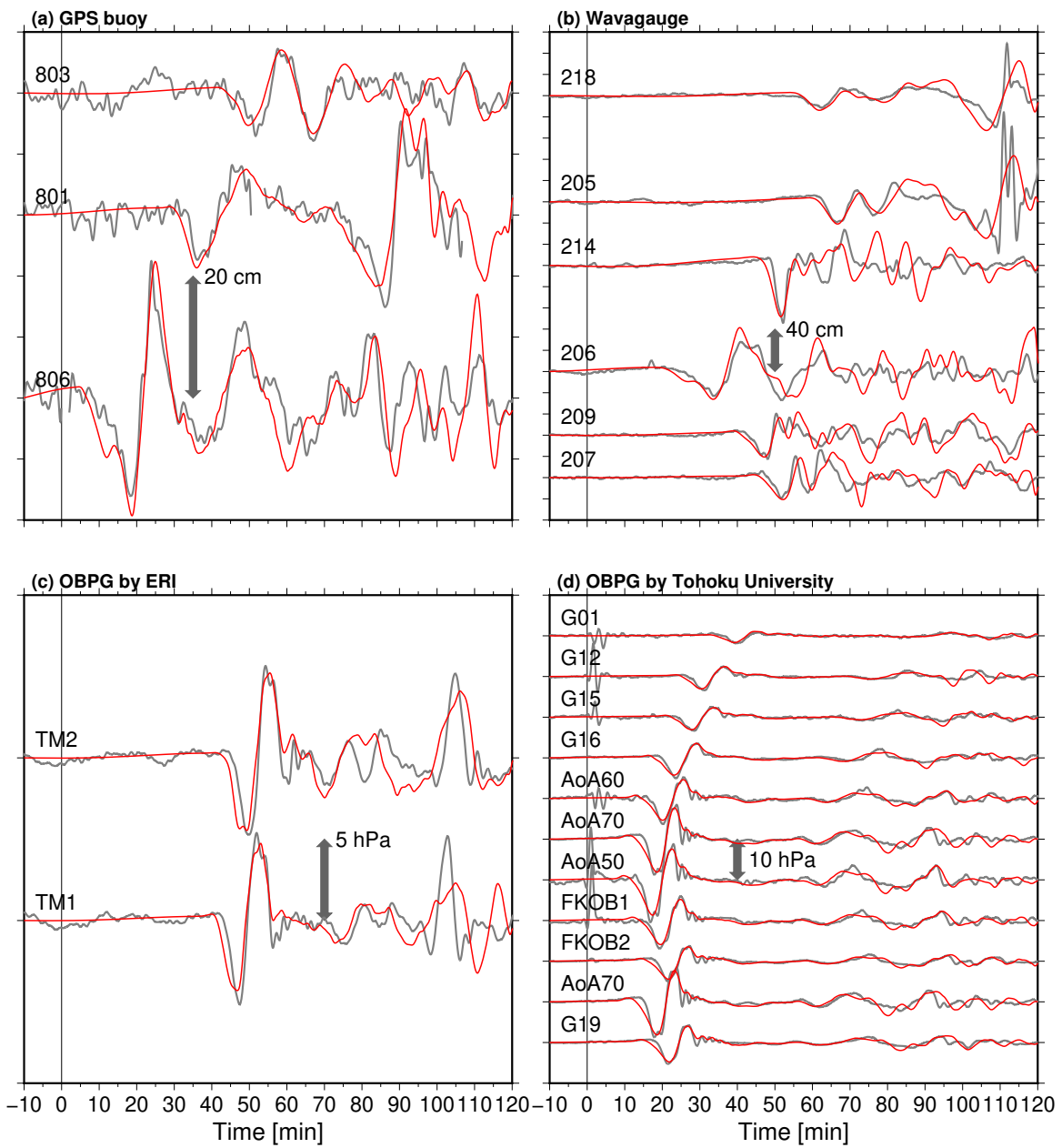
Figure S5. Waveform comparisons for the other tsunami stations from the finite fault model for (a) NOWPHAS Near-coastal GPS buoys, (b) NOWPHAS wave gauges, (c) OBPGs installed by ERI, and (d) OBPGs installed by Tohoku University. See Figure 1 for station locations.

1

Table S1. Search range for the grid search analysis.

Parameters	Range	Increment
Longitude [ab]	141.46°E ± 20 km	5 km
Latitude [ab]	37.31°N ± 20 km	5 km
Depth [ab]	12.0 km ± 10 km[a]	2 km
Strike [a]	49°	Fixed
Dip [a]	35°	Fixed
Rake [a]	−89°	Fixed
Length[c]	5 km – 60 km	5 km
Width[c]	5 km – 60 km	5 km
Slip amount	Adjusted so that the VR value takes the maximum	

[a]Reference values are taken from the GCMT solution.
[b]Fault center location is shown.
[c]When the depth of the updip end of the fault is shallower than a depth of 0.1 km, the calculation is skipped.

Table S2. Station list of the OBPGs installed by Tohoku University

Station	Longitude (°E)	Latitude (°N)	Depth (m)	Observation duration (yyyy/mm/dd)	Logger type[a]
G01	144.9204	38.7030	5456	2016/05/22 – 2017/04/11	UME
G12	143.5317	38.0213	4366	2016/05/24 – 2017/04/10	UME
G16	143.0470	37.3324	4414	2016/05/27 – 2017/04/15	HAK
G17[b]	142.7123	36.8979	4232	2016/05/28 – 2017/04/09	HAK
G19	142.6735	36.4931	5691	2016/05/28 – 2017/04/09	HAK
AoA50	142.3176	36.8725	2853	2016/09/22 – 2017/11/09	UME
AoA60[b]	142.7140	36.8993	4225	2016/09/22 – 2017/10/15	UME
AoA70	142.2868	36.6937	2544	2016/09/22 – 2017/10/15	HAK
FKOB1	142.5800	36.8055	4550	2016/09/28 – 2017/10/15	UME
FKOB2	142.8553	36.7225	5506	2016/09/28 – 2017/10/14	HAK
G15	143.5215	37.6773	5239	2016/10/02 – 2017/10/19	UME

[a]UME: Paroscientific Series 8CB intelligent type pressure sensor + Umezawa-Musen Co. data logger, HAK: Paroscientific Series 8B pressure sensor + Hakusan Co. LS9150 data logger
[b] Station G17 and AoA60 are installed at almost identical location.